Intra-cavity stimulated emissions of photons in almost pure spin states without imposed nonreciprocity

Shu-Wei Chang[1,2,*]

[1] *Research Center for Applied Sciences, Academia Sinica, Nankang, Taipei 11529, Taiwan*
[2] *Department of Photonics, National Chiao-Tung University, Hsinchu 30010, Taiwan*

*swchang@sinica.edu.tw

Abstract: We propose a chiral Fabry-Perot cavity in which only the cavity modes in almost pure spin (circular polarization) states lase in the presence of gain. In absence of imposed nonreciprocal environments and time-reversal symmetry breaking of emitter states to favor the emission of circularly-polarized photons, only the resonance of modes with a specific spin orientation remains in the cavity. We demonstrate a prototype of the cavity using distributed Bragg reflectors and cholesteric liquid crystals. This reciprocal cavity may provide a method to control the angular momentum state of emitters based on stimulated emissions.

OCIS codes: (260.5430) Polarization; (140.3430) Laser theory; (160.1585) Chiral media.

References and links

1. H. de Vries, "Rotatory power and other optical properties of certain liquid crystals," Acta. Cryst. **4**, 219–226 (1951).
2. C. Elachi and C. Yeh, "Stop bands for optical wave propagation in cholesteric liquid crystals," J. Opt. Soc. Am. **63**, 840–842 (1973).
3. L. Allen, M. W. Beijersbergen, R. J. C. Spreeuw, and J. P. Woerdman, "Orbital angular momentum of light and the transformation of Laguerre-Gaussian laser modes," Phys. Rev. A **45**, 8185–8189 (1992).
4. N. R. Heckenberg, R. McDuff, C. P. Smith, and A. G. White, "Generation of optical phase singularities by computer-generated holograms," Opt. Lett. **17**, 221–223 (1992).
5. M. W. Beijersbergen, R. P. C. Coerwinkel, M. Kristensen, and J. Woerdman, "Helical-wavefront laser beams produced with a spiral phaseplate," Opt. Commun. **112**, 321–327 (1994).
6. N. B. Simpson, K. Dholakia, L. Allen, and M. J. Padgett, "Optical helices and spiral interference fringes," Opt. Lett. **22**, 52–54 (1997).
7. L. Marrucci, C. Manzo, and D. Paparo, "Optical spin-to-orbital angular momentum conversion in inhomogeneous anisotropic media," Phys. Rev. Lett. **96**, 163905 (2006).
8. S. Franke-Arnold, L. Allen, and M. Padgett, "Advances in optical angular momentum," Laser Photon. Rev. **2**, 299–313 (2008).
9. A. M. Yao and M. J. Padgett, "Orbital angular momentum: origins, behavior and applications," Adv. Opt. Photon. **3**, 161–204 (2011).
10. R. A. Beth, "Mechanical detection and measurement of the angular momentum of light," Phys. Rev. **50**, 115–125 (1936).
11. H. He, M. E. J. Friese, N. R. Heckenberg, and H. Rubinsztein-Dunlop, "Direct observation of transfer of angular momentum to absorptive particles from a laser beam with a phase singularity," Phys. Rev. Lett. **75**, 826–829 (1995).
12. H. Ando, T. Sogawa, and H. Gotoh, "Photon-spin controlled lasing oscillation in surface-emitting lasers," Appl. Phys. Lett. **73**, 566–568 (1998).
13. H. Fujino, S. Koh, S. Iba, T. Fujimoto, and H. Kawaguchi, "Circularly polarized lasing in a (110)-oriented quantum well vertical-cavity surface-emitting laser under optical spin injection," Appl. Phys. Lett. **94**, 131108 (2009).

#158662 - $15.00 USD Received 23 Nov 2011; revised 11 Jan 2012; accepted 11 Jan 2012; published 19 Jan 2012

14. M. Holub, J. Shin, S. Chakrabarti, and P. Bhattacharya, "Electrically injected spin-polarized vertical-cavity surface-emitting lasers," Appl. Phys. Lett. **87**, 091108 (2005).
15. M. Holub, J. Shin, D. Saha, and P. Bhattacharya, "Electrical spin injection and threshold reduction in a semiconductor laser," Phys. Rev. Lett. **98**, 146603 (2007).
16. M. Holub and P. Bhattacharya, "Spin-polarized light-emitting diodes and lasers," J. Phys. D: Appl. Phys. **40**, R179–R203 (2007).
17. V. I. Kopp, B. Fan, H. K. M. Vithana, and A. Z. Genack, "Low-threshold lasing at the edge of a photonic stop band in cholesteric liquid crystals," Opt. Lett. **23**, 1707–1709 (1998).
18. B. Taheri, A. F. Munoz, P. Palffy-Muhoray, and R. Twieg, "Low threshold lasing in cholesteric liquid crystals," Mol. Cryst. Liq. Cryst. **358**, 73–82 (2001).
19. J. Schmidtke, W. Stille, H. Finkelmann, and S. T. Kim, "Laser emission in a dye doped cholesteric polymer network," Adv. Mater. **14**, 746 (2002).
20. H. Coles and S. Morris, "Liquid-crystal lasers," Nat. Photonics **4**, 676–685 (2010).
21. V. I. Kopp and A. Z. Genack, "Twist defect in chiral photonic structures," Phys. Rev. Lett. **89**, 033901 (2002).
22. J. Schmidtke, W. Stille, and H. Finkelmann, "Defect mode emission of a dye doped cholesteric polymer network," Phys. Rev. Lett. **90**, 083902 (2003).
23. J. Hwang, M. H. Song, B. Park, S. Nishimura, T. Toyooka, J. W. Wu, Y. Takanishi, K. Ishikawa, and H. Takezoe, "Electro-tunable optical diode based on photonic bandgap liquid-crystal heterojunctions," Nat. Mater. **4**, 383–387 (2005).
24. V. I. Kopp, Z. Q. Zhang, and A. Z. Genack, "Lasing in chiral photonic structures," Prog. Quantum Electron. **27**, 369–416 (2003).
25. K. Konishi, M. Nomura, N. Kumagai, S. Iwamoto, Y. Arakawa, and M. Kuwata-Gonokami, "Circularly polarized light emission from semiconductor planar chiral nanostructures," Phys. Rev. Lett. **106**, 057402 (2011).
26. Y. Matsuhisa, R. Ozaki, M. Ozaki, and K. Yoshino, "Single-mode lasing in one-dimensional periodic structure containing helical structure as a defect," Jpn. J. Appl. Phys. Part 2 **44**, L629–L632 (2005).
27. Y. Matsuhisa, Y. Huang, Y. Zhou, S. T. Wu, Y. Takao, A. Fujii, and M. Ozaki, "Cholesteric liquid crystal laser in a dielectric mirror cavity upon band-edge excitation," Opt. Express **15**, 616–622 (2007).
28. B. Park, M. Kim, S. W. Kim, and I. T. Kim, "Circularly polarized unidirectional lasing from a cholesteric liquid crystal layer on a 1-D photonic crystal substrate," Opt. Express **17**, 12323–12331 (2009).
29. H. A. Lorentz, "The theorem of poynting concerning the energy in the electromagnetic field and two general propositions concerning the propagation of light," Amsterdammer Akademie der Wetenschappen **4**, 176 (1896).
30. J. A. Kong, *Electromagnetic Wave Theory* (EMW Publishing, 2008), last ed.
31. S. W. Chang, "Full frequency-domain approach to reciprocal microlasers and nanolasers-perspective from Lorentz reciprocity," Opt. Express **19**, 21116–21134 (2011).
32. S. M. Barnett, B. Huttner, and R. Loudon, "Spontaneous emission in absorbing dielectric media," Phys. Rev. Lett. **68**, 3698–3701 (1992), (The dyadic Green's function in that work has a sign difference from that used here).
33. A. L. Shelankov and G. E. Pikus, "Reciprocity in reflection and transmission of light," Phys. Rev. B **46**, 3326–3336 (1992).
34. S. H. Friedberg, A. J. Insel, and L. E. Spence, *Linear Algebra* (Prentice Hall, 1989), 2nd ed.
35. P. J. W. Hands, C. A. Dobson, S. M. Morris, M. M. Qasim, D. J. Gardiner, T. D. Wilkinson, and H. J. Coles, "Wavelength-tuneable liquid crystal lasers from the visible to the near-infrared," Proc. SPIE **8114**, 81140T (2011).
36. D. W. Berreman, "Optics in smoothly varying anisotropic plannar structures: application to liquid-crystal twist cells," J. Opt. Soc. Am. **63**, 1374–1380 (1973).
37. S. L. Chuang, *Physics of Optoelectronic Devices* (Wiley and Sons, 1995), 1st ed.

1. Introduction

Nonvanishing angular momenta in quantum mechanical systems often come along with the time-reversal symmetry (T symmetry) breaking. For example, the Zeeman splitting of electron spin states requires a magnetic field which breaks the T symmetry. In optics, in addition to nonreciprocal responses such as the magneto-optic effect which distinguishes the two circular polarization (spin) states in a time-irreversible way, we gain another access to angular momenta of optical fields via reciprocal photonic structures. Such examples include quarter-wave plates which transform linearly polarized (LP) beams into circularly polarized (CP) ones, or cholesteric liquid crystals (CLCs) in the chiral phase that filter CP components of incident waves [1, 2]. Specific mask patterns can also transfer orbital angular momenta to optical beams [3–9]. In these schemes, the angular momentum difference between the incoming and outgoing beams is balanced by those of mechanical objects which may exhibit observable ro-

#158662 - $15.00 USD Received 23 Nov 2011; revised 11 Jan 2012; accepted 11 Jan 2012; published 19 Jan 2012

tations [10, 11] if they are not too bulky.

While the coherent CP radiation can be simply produced with proper placements of quarter-wave plates in front of LP lasers (spin-state designation after photons leave the cavity), it is more interesting to speculate another route: the immediate and almost perfect spin-state assignment of photons when photons are generated, namely, direct intra-cavity emissions of CP photons. The latter category brings about more understandings and perspectives to the matter-field interactions and related carrier (gain) dynamics. Such attempts could be carried out by preparing the excited levels of emitters in specific angular-momentum states, of which only one type of CP photons are emitted due to the angular-momentum conservation in the involved radiative transitions. Examples of this kind include the CP lasing due to spin-polarized carriers in vertical cavity surface emitting lasers through the spin-selective optical pumping [12, 13] or the spin-aligned electrical injection [14,15]. These schemes usually require explicit T-symmetry breaking (CP optical pump or magnetic spin aligner) to distinguish specific angular-momentum emitter states from others. However, the corresponding degree of circular polarization often depends critically on the operation temperature [16]. Another category is the CP radiation of dye-doped CLC bandedge [17–20] or defect lasers [20–23]. Nevertheless, it is not obvious that the direct and nearly pure spin assignment of photons is achieved in this case. Take bandedge CLC lasers as an example. The polarization profiles of the Bloch modes that experience the most gain from excited dye molecules are strongly coupled to the chiral structure of CLCs and resemble LP helices along the CLC helical axis [24]. The polarizations of lasing modes do not spin much inside the CLC cavity while the CP radiation is mainly decomposed from these modes at outputs. Therefore, the spin orientation of photons could not be viewed as directly set during emissions unambiguously.

The degree of circular polarization from CLC lasers, on the other hand, is more robust than that of the scheme based on external T-symmetry breaking because the circular polarization results from the less fragile photonic effect at room temperature. Despite the indirect spin assignment of emitted photons in the CLC case, chirality generally affects the spin and propagation (helicity) of photons. Experimentally, the photon emission from quantum dots coupling to the two CP radiation reservoirs through the planar chiral structure has been attempted [25]. Our concern is whether with chiral cavities, the high purity of photon spin states can be achieved directly as photons are emitted. If this condition is achievable, we may control the angular-momentum states of emitters without imposed T-symmetry breaking such as an external magnetic field. Note that in *reciprocal* (or *time-reversal invariant* without loss or gain) cavities, spontaneous emissions (SPEs) cannot distinguish pairs of time-reversal states. However, the stimulated emissions (STEs) can do the job. This point will be addressed in section 2.

In this paper, we present a one-dimensional (1D) Fabry-Perot (FP) chiral cavity which exhibits significant intra-cavity CP photon emissions when lasing. Under certain criteria, the polarizations of the two lasing modes turn into the same spin state while the other spin state has no cavity resonance associated with it. As a result, only one circular polarization stands out in the presence of gain. We show that such a FP laser is realizable using isotropic distributed Bragg reflectors (DBRs) and CLCs, of which a few combinations had been considered in literature [26–28]. With an isotropic gain and randomly oriented dipole currents perpendicular to the propagation axis of the FP cavity, both of which do not favor particular CP emissions, we show that CP photon emissions are indeed due to chirality only.

In the remaining part of this paper, we first define reciprocal cavities and discuss the relation of spontaneous and stimulated emissions to T-symmetry breaking in these cavities (section 2). The features of FP cavities utilizing a unique type of chiral reflectors are then discussed, and we will show how to characterize the polarization state of the intra-cavity field with the 1D dyadic Green's function and Stokes parameters (section 3). A prototype of the chiral FP

#158662 - $15.00 USD Received 23 Nov 2011; revised 11 Jan 2012; accepted 11 Jan 2012; published 19 Jan 2012

cavity using CLCs and DBRs will be demonstrated, and the intra-cavity Stokes parameters are calculated to verify that the lasing mode is indeed significantly circularly-polarized inside the cavity (section 4). Although we begin with a reciprocal condition, we show that the feedback from CP stimulated emissions may turn the cavity nonreciprocal (section 5). A conclusion will be given at the end (section 6).

2. Time-reversal symmetry breaking from photon emissions in reciprocal cavities

A reciprocal cavity is a resonance structure (assuming a relative permeability of unity) in which two current sources $\mathbf{J}_{\mathrm{s},1}(\mathbf{r},\omega)$ and $\mathbf{J}_{\mathrm{s},2}(\mathbf{r},\omega)$ and the corresponding electric fields $\mathbf{E}_1(\mathbf{r},\omega)$ and $\mathbf{E}_2(\mathbf{r},\omega)$ oscillating at a frequency ω satisfy the Lorentz reciprocity theorem in the regime of linear optics [29, 30]:

$$\int_\Omega \mathrm{d}\mathbf{r}\mathbf{J}_{\mathrm{s},1}(\mathbf{r},\omega)\cdot\mathbf{E}_2(\mathbf{r},\omega)=\int_\Omega \mathrm{d}\mathbf{r}\mathbf{J}_{\mathrm{s},2}(\mathbf{r},\omega)\cdot\mathbf{E}_1(\mathbf{r},\omega), \tag{1}$$

where Ω is a region outside which $\mathbf{J}_{\mathrm{s},1}(\mathbf{r},\omega)$ and $\mathbf{J}_{\mathrm{s},2}(\mathbf{r},\omega)$ vanish. A nonreciprocal cavity is the one in which the integral identity in Eq. (1) does not hold. Violations of the theorem occur when the permeability tensor $\overline{\overline{\varepsilon}}_{\mathrm{r}}(\mathbf{r},\omega)$ represented in a real orthonormal basis set (for example $\hat{x}$, $\hat{y}$, and $\hat{z}$) is nonsymmetric, namely $\overline{\overline{\varepsilon}}_{\mathrm{r}}(\mathbf{r},\omega)\neq\overline{\overline{\varepsilon}}_{\mathrm{r}}^{\mathrm{T}}(\mathbf{r},\omega)$, where the superscript "T" means matrix transpose. Thus, we classify the cavity as reciprocal or nonreciprocal based on whether $\overline{\overline{\varepsilon}}_{\mathrm{r}}(\mathbf{r},\omega)$ is symmetric [30, 31]. For the nonlinear regime such as lasers, we generalize this criterion of symmetric matrices to the effective permittivity tensor dressed by nonlinearities [31]. Note that the term (non)reciprocal here refers to the validity of the Lorenz reciprocity theorem rather than certain distinct behaviors of specifically-polarized waves which still satisfy Eq. (1) [23].

In reciprocal cavities, spontaneous emissions cannot break the T symmetry of emitter states by distinguishing the occupation number of one of the time-reversal paired states from the other. To see that, let us compare the SPE rate $R_{\mathrm{sp},cv}$ between states c and v (apart from a local correction factor due to dielectric constituents) [32] with that $R_{\mathrm{sp},\tilde{c}\tilde{v}}$ between the time-reversal states $\tilde{c}$ and $\tilde{v}$ at the same location $\mathbf{r}_{\mathrm{s}}$ in a reciprocal cavity:

$$\begin{aligned}R_{\mathrm{sp},cv}-R_{\mathrm{sp},\tilde{c}\tilde{v}}&=\frac{2\mu_0\omega_{cv}^2}{\hbar}\mathrm{Im}\left[\boldsymbol{\mu}_{vc}^*\cdot\overline{\overline{G}}_{\mathrm{ee}}(\mathbf{r}_{\mathrm{s}},\mathbf{r}_{\mathrm{s}},\omega_{cv})\boldsymbol{\mu}_{vc}\right]-\frac{2\mu_0\omega_{\tilde{c}\tilde{v}}^2}{\hbar}\mathrm{Im}\left[\boldsymbol{\mu}_{\tilde{v}\tilde{c}}^*\cdot\overline{\overline{G}}_{\mathrm{ee}}(\mathbf{r}_{\mathrm{s}},\mathbf{r}_{\mathrm{s}},\omega_{\tilde{c}\tilde{v}})\boldsymbol{\mu}_{\tilde{v}\tilde{c}}\right]\\&=\frac{2\mu_0\omega_{cv}^2}{\hbar}\mathrm{Im}\left[\boldsymbol{\mu}_{vc}^*\cdot\left\{\overline{\overline{G}}_{\mathrm{ee}}(\mathbf{r}_{\mathrm{s}},\mathbf{r}_{\mathrm{s}},\omega_{cv})-\overline{\overline{G}}_{\mathrm{ee}}^{\mathrm{T}}(\mathbf{r}_{\mathrm{s}},\mathbf{r}_{\mathrm{s}},\omega_{\tilde{c}\tilde{v}})\right\}\boldsymbol{\mu}_{vc}\right]=0,\end{aligned} \tag{2}$$

where μ_o is the vacuum permittivity; $\hbar$ is the Planck constant divided by 2π; $\boldsymbol{\mu}_{vc}$ and ω_{cv} ($\boldsymbol{\mu}_{\tilde{v}\tilde{c}}$ and $\omega_{\tilde{c}\tilde{v}}$) are the dipole moment and transition frequency between states c and v ($\tilde{c}$ and $\tilde{v}$), respectively ($\boldsymbol{\mu}_{\tilde{v}\tilde{c}}=\boldsymbol{\mu}_{vc}^*$ up to a constant phase; and $\omega_{cv}=\omega_{\tilde{c}\tilde{v}}$ in absence of T-symmetry breaking); $\overline{\overline{G}}_{\mathrm{ee}}(\mathbf{r},\mathbf{r}',\omega)$ is the dyadic Green's function at frequency ω, which connects the current density at $\mathbf{r}'$ to the optical field at $\mathbf{r}$ and exhibits the symmetry property $\overline{\overline{G}}_{\mathrm{ee}}(\mathbf{r},\mathbf{r}',\omega)=\overline{\overline{G}}_{\mathrm{ee}}^{\mathrm{T}}(\mathbf{r}',\mathbf{r},\omega)$ (represented in a real orthonormal basis set) in a reciprocal environment; and we have used the fact that for a scalar X, $X=X^{\mathrm{T}}$. From Eq. (2), if the initial occupation probabilities of states c and v are identical to those of $\tilde{c}$ and $\tilde{v}$, respectively, spontaneous emissions cannot make their occupations uneven at later times.

On the other hand, from Poynting's theorem, the STE rates $R_{\mathrm{st},cv}$ and $R_{\mathrm{st},\tilde{c}\tilde{v}}$ triggered by the two transitions in the same cavity could be different. Let us look into the difference between the two transition rates:

$$\begin{aligned}R_{\mathrm{st},cv}-R_{\mathrm{st},\tilde{c}\tilde{v}}&=\frac{\varepsilon_0}{2\hbar}\int\mathrm{d}\mathbf{r}'\mathrm{Im}\left[\mathbf{E}_{vc}(\mathbf{r}')\cdot\Delta\overline{\overline{\varepsilon}}_{\mathrm{r,a}}^*(\mathbf{r}',\omega_{cv})\mathbf{E}_{vc}^*(\mathbf{r}')-\mathbf{E}_{\tilde{v}\tilde{c}}(\mathbf{r}')\cdot\Delta\overline{\overline{\varepsilon}}_{\mathrm{r,a}}^*(\mathbf{r}',\omega_{\tilde{c}\tilde{v}})\mathbf{E}_{\tilde{v}\tilde{c}}^*(\mathbf{r}')\right]\\&=\frac{2\varepsilon_0\mu_0^2\omega_{cv}^4}{\hbar}\int\mathrm{d}\mathbf{r}'\mathscr{R}_{\mathrm{st},cv,\tilde{c}\tilde{v}}(\mathbf{r}',\mathbf{r}_{\mathrm{s}}),\end{aligned} \tag{3a}$$

#158662 - $15.00 USD Received 23 Nov 2011; revised 11 Jan 2012; accepted 11 Jan 2012; published 19 Jan 2012

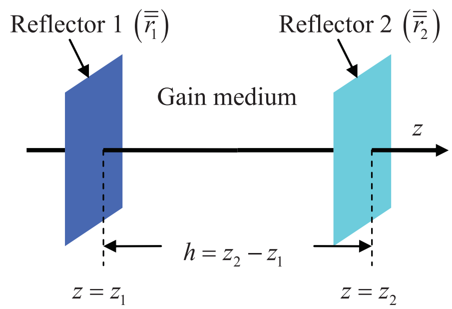

Fig. 1. The schematic diagram of the 1D FP cavity. Reflector 1 is isotropic while reflector 2 is chiral with specific characteristics of reflections.

$$\begin{aligned}\mathscr{R}_{\mathrm{st},cv,\tilde{c}\tilde{v}}(\mathbf{r}',\mathbf{r}_\mathrm{s}) = \mathrm{Im}\Big[\boldsymbol{\mu}_{vc}^{*}\cdot\big\{&\overline{\overline{G}}_\mathrm{ee}^{\dagger}(\mathbf{r}',\mathbf{r}_\mathrm{s},\omega_{cv})\Delta\overline{\overline{\varepsilon}}_\mathrm{r,a}^{\dagger}(\mathbf{r}',\omega_{cv})\overline{\overline{G}}_\mathrm{ee}(\mathbf{r}',\mathbf{r}_\mathrm{s},\omega_{cv})\\ &-\overline{\overline{G}}_\mathrm{ee}^{\mathrm{T}}(\mathbf{r}',\mathbf{r}_\mathrm{s},\omega_{cv})\Delta\overline{\overline{\varepsilon}}_\mathrm{r,a}^{*}(\mathbf{r}',\omega_{cv})\overline{\overline{G}}_\mathrm{ee}^{*}(\mathbf{r}',\mathbf{r}_\mathrm{s},\omega_{cv})\big\}\boldsymbol{\mu}_{vc}\Big],\end{aligned} \quad (3b)$$

where ε_0 is the vacuum permittivity; $\mathscr{R}_{\mathrm{st},cv,\tilde{c}\tilde{v}}(\mathbf{r}',\mathbf{r}_\mathrm{s})$ is an integrand proportional to the difference between two local transition-rate densities at $\mathbf{r}'$; "†" means hermitian conjugates of matrices; $\Delta\overline{\overline{\varepsilon}}_\mathrm{r,a}(\mathbf{r}',\omega)$ is the variation of the permittivity tensor due to the presence of gain and is symmetric when represented in a real orthonormal basis set $[\Delta\overline{\overline{\varepsilon}}_\mathrm{r,a}^{\mathrm{T}}(\mathbf{r}',\omega) = \Delta\overline{\overline{\varepsilon}}_\mathrm{r,a}(\mathbf{r}',\omega)]$ in reciprocal environments; and $\mathbf{E}_{vc}(\mathbf{r}')$ $[\mathbf{E}_{\tilde{v}\tilde{c}}(\mathbf{r}')]$ is the field generated by $\boldsymbol{\mu}_{vc}$ $(\boldsymbol{\mu}_{\tilde{v}\tilde{c}})$:

$$\mathbf{E}_{vc(\tilde{v}\tilde{c})}(\mathbf{r}') = 2\mu_0\omega_{cv(\tilde{c}\tilde{v})}^2\overline{\overline{G}}_\mathrm{ee}(\mathbf{r}',\mathbf{r}_s,\omega_{cv(\tilde{c}\tilde{v})})\boldsymbol{\mu}_{vc(\tilde{v}\tilde{c})}. \quad (3c)$$

Further applying the symmetric form of the reciprocal dyadic Green's function to Eq. (3b) and assuming an isotropic gain $[\Delta\overline{\overline{\varepsilon}}_\mathrm{r,a}(\mathbf{r}',\omega) = i\Delta\varepsilon_\mathrm{r,a,I}(\mathbf{r}',\omega)\overline{\overline{I}}_3$, where $\Delta\varepsilon_\mathrm{r,a,I}(\mathbf{r}',\omega)$ describes the isotropic gain; and $\overline{\overline{I}}_3$ is the 3-by-3 identity matrix], we simplify $\mathscr{R}_{\mathrm{st},cv,\tilde{c}\tilde{v}}(\mathbf{r}',\mathbf{r}_\mathrm{s})$ in Eq. (3b) as

$$\mathscr{R}_{\mathrm{st},cv,\tilde{c}\tilde{v}}(\mathbf{r}',\mathbf{r}_\mathrm{s}) = -2\Delta\varepsilon_\mathrm{r,a,I}(\mathbf{r}',\omega_{cv})\mathrm{tr}\left\{\mathrm{Im}\left[\overline{\overline{G}}_\mathrm{ee}(\mathbf{r}_\mathrm{s},\mathbf{r}',\omega_{cv})\overline{\overline{G}}_\mathrm{ee}^{*}(\mathbf{r}',\mathbf{r}_\mathrm{s},\omega_{cv})\right]\mathrm{Im}\left[\boldsymbol{\mu}_{vc}\boldsymbol{\mu}_{vc}^{\dagger}\right]\right\}, \quad (3d)$$

where "tr" means the trace sum. In Eq. (3d), the tensor product $\overline{\overline{G}}_\mathrm{ee}(\mathbf{r}_\mathrm{s},\mathbf{r}',\omega_{cv})\overline{\overline{G}}_\mathrm{ee}^{*}(\mathbf{r}',\mathbf{r}_\mathrm{s},\omega_{cv})$ [identical to $\overline{\overline{G}}_\mathrm{ee}(\mathbf{r}_\mathrm{s},\mathbf{r}',\omega_{cv})\overline{\overline{G}}_\mathrm{ee}^{\dagger}(\mathbf{r}_\mathrm{s},\mathbf{r}',\omega_{cv})$] is a hermitian matrix. If this product is real hermitian, the integrand $\mathscr{R}_{\mathrm{st},cv,\tilde{c}\tilde{v}}(\mathbf{r}',\mathbf{r}_\mathrm{s})$ always vanishes. On the other hand, in chiral (anisotropic) but reciprocal cavities, this product can be complex hermitian, leading to nonzero $\mathscr{R}_{\mathrm{st},cv,\tilde{c}\tilde{v}}(\mathbf{r}',\mathbf{r}_\mathrm{s})$. In particular, the nonvanishing integrand $\mathscr{R}_{\mathrm{st},cv,\tilde{c}\tilde{v}}(\mathbf{r}_\mathrm{s},\mathbf{r}_\mathrm{s})$ at $\mathbf{r}' = \mathbf{r}_\mathrm{s}$ means that the transition rate densities of $\boldsymbol{\mu}_{vc}$ and $\boldsymbol{\mu}_{\tilde{v}\tilde{c}}$ feedback by the corresponding dipole-induced fields (self-triggered STEs) may be different even with identical initial occupations of states c and $\tilde{c}$ (v and $\tilde{v}$). Physically, this phenomenon originates from the dipole-triggered lasing mode which carries a net angular momentum inside the cavity. In the next section, we will describe how to construct FP cavities of this type with a nearly perfect intra-cavity CP field when lasing.

3. Fabry-Perot cavities with a special chiral reflector

To construct FP cavities with a nearly perfect intra-cavity CP field, we incorporate the chirality into the reflector at one side of the cavity. Figure 1 shows the schematic diagram of the 1D FP cavity with a length h. The FP cavity is filled with an isotropic gain medium in the region $z \in (z_1, z_2)$. Reflector 1 (2) characterized by the reflection matrix $\overline{\overline{r}}_1$ ($\overline{\overline{r}}_2$) in the LP basis ($\hat{x}$ and $\hat{y}$) is located at z_1 (z_2). These matrices connect the cartesian components of the incident wave to

#158662 - $15.00 USD Received 23 Nov 2011; revised 11 Jan 2012; accepted 11 Jan 2012; published 19 Jan 2012

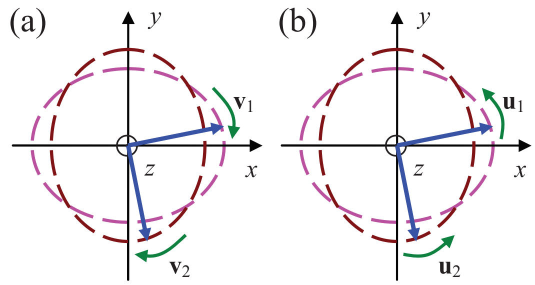

Fig. 2. The polarization states (a) $\mathbf{v}_{1,2}$ (case I), and (b) $\mathbf{u}_{1,2}$ (case II) when $\kappa \neq 0$. The phase angle of κ is set to $\arg(\sqrt{a-b})$. When $\kappa = 0$, the polarization states $\mathbf{v}_{1,2}$ become $\hat{e}_-$ while $\mathbf{u}_{1,2}$ turn into $\hat{e}_+$.

those of the reflected one. We set reflector 1 isotropic and adopt a special design for reflector 2. The reciprocity requires $\overline{\overline{r}}_2$ (matrix elements indexed by x, y) to be symmetric [33]:

$$\overline{\overline{r}}_2 \equiv \begin{pmatrix} r_{2,xx}, & r_{2,xy} \\ r_{2,yx}, & r_{2,yy} \end{pmatrix} = \begin{pmatrix} a, & c \\ c, & b \end{pmatrix}, \tag{4}$$

where a, b, and c are complex numbers. The reflection matrix $\overline{\overline{r}}_{2,\mathrm{CP}}$ in the CP basis [matrix elements indexed by $\pm$ corresponding to the basis $\hat{e}_\pm = (\hat{x} \pm i\hat{y})/\sqrt{2}$] is transformed from $\overline{\overline{r}}_2$ with the change of basis:

$$\overline{\overline{r}}_{2,\mathrm{CP}} \equiv \begin{pmatrix} r_{2,\mathrm{CP},++}, & r_{2,\mathrm{CP},+-} \\ r_{2,\mathrm{CP},-+}, & r_{2,\mathrm{CP},--} \end{pmatrix} = \overline{\overline{p}}^{\dagger}\,\overline{\overline{r}}_2\,\overline{\overline{p}} = \begin{pmatrix} \frac{a+b}{2}, & \frac{a-b}{2} - ic \\ \frac{a-b}{2} + ic, & \frac{a+b}{2} \end{pmatrix}, \tag{5a}$$

$$\overline{\overline{p}} = \begin{pmatrix} 1/\sqrt{2}, & 1/\sqrt{2} \\ i/\sqrt{2}, & -i/\sqrt{2} \end{pmatrix}, \tag{5b}$$

where $\overline{\overline{p}}$ is a unitary matrix describing the transformation between CP and LP representations.

The polarization states of cavity modes are closely related to eigenvectors of $\overline{\overline{r}}_2$ ($\overline{\overline{r}}_{2,\mathrm{CP}}$). Let us consider two special cases that one of the off-diagonal matrix elements in $\overline{\overline{r}}_{2,\mathrm{CP}}$ is much less significant than the other, namely, $(a-b)/2 \mp ic = \kappa^2$ ($-,+$ for case I, II) and $|\kappa|^2 \ll |a-b|$. In both cases, we solve the eigenvalue problem $\overline{\overline{r}}_{2,\mathrm{CP}}\mathbf{w} = \Lambda\mathbf{w}$ and obtain identical sets of eigenvalues Λ:

$$\Lambda = \Lambda_{1,2} = \frac{(a+b)}{2} \pm \kappa\sqrt{(a-b)-\kappa^2} \;\; (1,2 \text{ for } +,-). \tag{6a}$$

The eigenvectors $\mathbf{w}$ corresponding to case I (II) are denoted as $\mathbf{v}_{\mathrm{CP}}^{1,2}$ ($\mathbf{u}_{\mathrm{CP}}^{1,2}$) and written as

$$\mathbf{w} = \mathbf{v}_{\mathrm{CP}}^{1,2} = \begin{pmatrix} v_{\mathrm{CP},+}^{1,2} \\ v_{\mathrm{CP},-}^{1,2} \end{pmatrix} = \frac{1}{D(a,b,\kappa)} \begin{pmatrix} \pm\kappa \\ \sqrt{(a-b)-\kappa^2} \end{pmatrix} \;\; (\text{case I}), \tag{6b}$$

$$\mathbf{w} = \mathbf{u}_{\mathrm{CP}}^{1,2} = \begin{pmatrix} u_{\mathrm{CP},+}^{1,2} \\ u_{\mathrm{CP},-}^{1,2} \end{pmatrix} = \frac{1}{D(a,b,\kappa)} \begin{pmatrix} \sqrt{(a-b)-\kappa^2} \\ \pm\kappa \end{pmatrix} \;\; (\text{case II}), \tag{6c}$$

where $D(a,b,\kappa) = \sqrt{|\kappa|^2 + |(a-b)-\kappa^2|}$. As shown in Figs. 2(a) and 2(b), when $\kappa \neq 0$ [phase angle of κ is set to $\arg(\sqrt{a-b})$], the polarization eigenvectors $\mathbf{v}_{1,2} = v_{\mathrm{CP},+}^{1,2}\hat{e}_+ + v_{\mathrm{CP},-}^{1,2}\hat{e}_-$ ($\mathbf{u}_{1,2} =$

#158662 - $15.00 USD Received 23 Nov 2011; revised 11 Jan 2012; accepted 11 Jan 2012; published 19 Jan 2012

$u^{1,2}_{\mathrm{CP},+}\hat{e}_+ + u^{1,2}_{\mathrm{CP},-}\hat{e}_-$) of $\overline{\overline{r}}_2$ are two clockwise (counterclockwise) elliptical polarizations which resemble $\hat{e}_-$ ($\hat{e}_+$). When $\kappa = 0$, the two elliptical polarizations $\mathbf{v}_{1,2}$ ($\mathbf{u}_{1,2}$) become the identical circular polarization $\hat{e}_-$ ($\hat{e}_+$) with degenerate eigenvalues $\Lambda_{1,2} = (a+b)/2$. In this condition, the reflection matrix $\overline{\overline{r}}_{2,\mathrm{CP}}$ ($\overline{\overline{r}}_2$) is turned into the Jordan canonical form [34]. The two identical eigenvectors only represent one degree of freedom, while the other one has to be manually introduced. In the case of $\overline{\overline{r}}_{2,\mathrm{CP}}$ here, the remaining degree of freedom corresponds to one of the circular polarizations.

The polarization state of the field inside the FP cavity could be an almost pure spin state if the cavity modes carrying any of the two polarizations $\mathbf{v}_{1,2}$ ($\mathbf{u}_{1,2}$) are amplified. It does not matter which of $\mathbf{v}_{1,2}$ ($\mathbf{u}_{1,2}$) becomes the dominant polarization because they both resemble $\hat{e}_-$ ($\hat{e}_+$). To maintain the polarization eigenstates of reflector 2 throughout the FP cavity, isotropic reflector 1 is therefore adopted. In addition to these considerations, two issues still require clarifications. First, the two polarization eigenvectors $\mathbf{v}_{1,2}$ ($\mathbf{u}_{1,2}$) are linearly independent unless κ is strictly zero. Whenever $\kappa \neq 0$, photons might have tended to be emitted in a combined polarization state of $\mathbf{v}_{1,2}$ ($\mathbf{u}_{1,2}$) which carries no spin angular momentum. This point can be resolved with the Stokes parameter $S_3(z,\omega)$ inside the cavity, which is an indicator on the degree of circular polarization. Second, we need a prototype of reflector 2 to validate the feasibility of the concept in principle. Both issues will be addressed in section 4.

To see whether a nearly perfect CP field indeed exists inside the FP cavity with gain, we consider a SPE source $\mathbf{J}_\mathrm{s}(z,\omega)$ which only has the in-plane (xy) components relevant to the transverse polarization state and satisfies the following ensemble average:

$$\langle J^*_{\mathrm{s},\alpha'}(z',\omega) J_{\mathrm{s},\alpha}(z,\omega)\rangle = \delta_{\alpha'\alpha}\delta(z-z')\sum_{c,v} D^{cv}(z,\omega)\frac{|j_{\mathrm{sp},vc}(\omega)|^2}{2}, \tag{7}$$

where $\alpha',\alpha = x,y$; $D^{cv}(z,\omega)$ is the dipole density due to the radiative transition between states c and v, which contains the information of state filling and is only present inside the cavity; and $j_{\mathrm{sp},vc}(\omega)$ is the amplitude of the SPE dipole current. For simplicity, only the randomness of the SPE source along the z direction [$\delta(z-z')$ in Eq. (7)] is taken into account, which is pertinent to the fundamental transverse mode of typical FP lasers. The Kronecker delta $\delta_{\alpha'\alpha}$ indicates that the SPE source does not favor emissions in specific transverse polarization states. In the case of equal amounts of opposite-oriented but uncorrelated CP dipoles (no T-symmetry breaking), the form of the ensemble average remains identical to that in Eq. (7). Therefore, the polarization state of the intra-cavity lasing field is determined by the cavity alone. The optical field $\mathbf{E}(z,\omega)$ is connected to the SPE source through a response integral:

$$\mathbf{E}(z,\omega) = \int_{z_1}^{z_2} \mathrm{d}z' \overline{\overline{G}}_{\mathrm{ee}}(z,z',\omega) i\omega\mu_0 \mathbf{J}_\mathrm{s}(z',\omega), \tag{8a}$$

where the dyadic Green's function $\overline{\overline{G}}_{\mathrm{ee}}(z,z',\omega)$ is a 2-by-2 tensor now because only the in-plane components are considered. This Green's function $\overline{\overline{G}}_{\mathrm{ee}}(z,z',\omega)$ satisfies the reflection boundary conditions at z_1 and z_2 and can be analytically expressed in terms of two dyadic response kernels $\overline{\overline{G}}^{<}_{\mathrm{ee}}(z,z',\omega)$ [$z \in (z_1,z')$] and $\overline{\overline{G}}^{>}_{\mathrm{ee}}(z,z',\omega)$ [$z \in (z',z_2)$] in different regions:

$$\overline{\overline{G}}_{\mathrm{ee}}(z,z',\omega) = U(z'-z)\overline{\overline{G}}^{<}_{\mathrm{ee}}(z,z',\omega) + U(z-z')\overline{\overline{G}}^{>}_{\mathrm{ee}}(z,z',\omega), \tag{8b}$$

$$\begin{aligned}\overline{\overline{G}}^{<}_{\mathrm{ee}}(z,z',\omega) = \frac{\eta e^{ikh}}{2i\omega\mu_0}&\left[e^{ik(z-z_1)}\overline{\overline{r}}_1 + e^{-ik(z-z_1)}\overline{\overline{I}}_2\right]\left[\overline{\overline{r}}_2\overline{\overline{r}}_1 e^{2ikh} - \overline{\overline{I}}_2\right]^{-1}\\ &\times\left[e^{-ik(z'-z_2)}\overline{\overline{r}}_2 + e^{ik(z'-z_2)}\overline{\overline{I}}_2\right],\end{aligned} \tag{8c}$$

#158662 - $15.00 USD Received 23 Nov 2011; revised 11 Jan 2012; accepted 11 Jan 2012; published 19 Jan 2012

$$\overline{\overline{G}}^{>}_{\rm ee}(z,z',\omega) = \frac{\eta e^{ikh}}{2i\omega\mu_0}\left[e^{-ik(z-z_2)}\overline{\overline{r}}_2 + e^{ik(z-z_2)}\overline{\overline{I}}_2\right]\left[\overline{\overline{r}}_1\overline{\overline{r}}_2 e^{2ikh} - \overline{\overline{I}}_2\right]^{-1} \times \left[e^{ik(z'-z_1)}\overline{\overline{r}}_1 + e^{-ik(z'-z_1)}\overline{\overline{I}}_2\right], \tag{8d}$$

where $U(z)$ is the Heaviside step function [$U(z) = 1$ if $z > 0$; 0 otherwise]; η is the impedance of the gain medium; and k is the complex propagation constant incorporating the gain effect.

The spectra of the four Stokes parameters $S_n(z,\omega)$ ($n = 0-3$) inside the cavity are then calculated from $\mathbf{E}(z,\omega)$ [33]:

$$S_n(z,\omega) = \mathbf{E}^*(z,\omega)\cdot\overline{\overline{M}}_n\mathbf{E}(z,\omega), \tag{9}$$

where $\overline{\overline{M}}_0 = \overline{\overline{I}}_2$ (2-by-2 identity matrix), $\overline{\overline{M}}_1 = \overline{\overline{\sigma}}_3$, $\overline{\overline{M}}_2 = \overline{\overline{\sigma}}_1$, $\overline{\overline{M}}_3 = \overline{\overline{\sigma}}_2$ [$\overline{\overline{\sigma}}_n$ ($n = 1-3$) are Pauli matrices]. The parameter $S_0(z,\omega)$ represents the intensity of the field. While $S_1(z,\omega)$ and $S_2(z,\omega)$ are both the intensity differences of the two orthogonal LP components, $S_3(z,\omega)$ reveals how significant a CP component is. To obtain the polarization state inside the FP cavity, we substitute the expressions of $\mathbf{E}(z,\omega)$ and $\overline{\overline{G}}_{\rm ee}(z,z',\omega)$ in Eq. (8a) to (8d) into the Stokes parameters in Eq. (9) and then take the ensemble average $\langle S_n(z,\omega)\rangle$ with the aid of Eq. (7). For a perfect CP field, the magnitude $|\langle S_3(z,\omega)\rangle|$ is equal to $\langle S_0(z,\omega)\rangle$ while $\langle S_1(z,\omega)\rangle$ and $\langle S_2(z,\omega)\rangle$ vanish. If we further assume that the dipole density $D^{cv}(z,\omega)$ is uniform (valid for short cavities), and the amplitude of SPE source $j_{{\rm sp},vc}(\omega)$ and $D^{cv}(z,\omega)$ are frequency-independent, the dominant frequency dependence of the Stokes parameter $\langle S_n(z,\omega)\rangle$ comes from an integral $\mathscr{I}_n(z,\omega)$ defined as

$$\mathscr{I}_n(z,\omega) \equiv \int_{z_1}^{z_2} {\rm d}z'\,{\rm tr}\left[\overline{\overline{G}}_{\rm ee}(z,z',\omega)\overline{\overline{G}}^{\dagger}_{\rm ee}(z,z',\omega)\overline{\overline{M}}_n\right]. \tag{10}$$

The integral $\mathscr{I}_n(z,\omega)$ can be calculated analytically with the expression of $\overline{\overline{G}}_{\rm ee}(z,z',\omega)$ in Eq. (8b) to (8d). Note that if we apply the reciprocity condition $\overline{\overline{G}}^{\dagger}_{\rm ee}(z,z',\omega) = \overline{\overline{G}}^{*}_{\rm ee}(z',z,\omega)$ in Eq. (10), the integrand ${\rm tr}[\overline{\overline{G}}_{\rm ee}(z,z',\omega)\overline{\overline{G}}^{\dagger}_{\rm ee}(z,z',\omega)\overline{\overline{M}}_3]$ in $\mathscr{I}_3(z,\omega)$, which describes the degree of circular polarization, is closely related to $\mathscr{R}_{{\rm st},cv,\tilde{c}\tilde{v}}(z',z)$ in Eq. (3d) when $\boldsymbol{\mu}_{vc} = |\boldsymbol{\mu}_{vc}|\hat{e}_+$ is a CP dipole moment in a homogeneous active region:

$$\mathscr{R}_{{\rm st},cv,\tilde{c}\tilde{v}}(z',z) \propto {\rm Re}\left[{\rm tr}\left\{\overline{\overline{G}}_{\rm ee}(z,z',\omega)\overline{\overline{G}}^{\dagger}_{\rm ee}(z,z',\omega)\overline{\overline{M}}_3\right\}\right]\Big|_{\omega=\omega_{cv}}. \tag{11}$$

If we integrate both sides of Eq. (11) over z' in the active region [$z' \in (z_1,z_2)$] with a homogeneous gain, the real parts ${\rm Re}[\mathscr{I}_3(z_{\rm s},\omega_{cv})]$ and ${\rm Re}[\langle S_3(z_{\rm s},\omega_{cv})\rangle]$ ($z_{\rm s}$ is the z coordinate of the dipole moment $\boldsymbol{\mu}_{vc}$) turn out to be proper indicators of the difference $R_{{\rm st},cv} - R_{{\rm st},\tilde{c}\tilde{v}}$ between two dipole-triggered STE rates which are related to each other via the T symmetry in Eq. (3a).

The resonance effect of the FP cavity is also one of the causes to the potential CP field. When reflector 1 is isotropic ($\overline{\overline{r}}_1 = \Gamma\overline{\overline{I}}_2$, where Γ is the reflection coefficient), the dyadic Green's function $\overline{\overline{G}}_{\rm ee}(z,z',\omega)$ is a matrix function of $\overline{\overline{r}}_2$ only, as indicated by Eq. (8b) to (8d). Thus, the polarizations $\mathbf{v}_{1,2}$ ($\mathbf{u}_{1,2}$) are also the eigenvectors of $\overline{\overline{G}}_{\rm ee}(z,z',\omega)$. In particular, the dyadic Green's function $\overline{\overline{G}}_{\rm ee}(z,z',\omega)$ contains a matrix $[\Gamma\exp(2ikh)\overline{\overline{r}}_2 - \overline{\overline{I}}_2]^{-1}$, and the operation of $\overline{\overline{G}}_{\rm ee}(z,z',\omega)$ on $\mathbf{v}_{1,2}$ (take case I for example) leads to an eigenstate relation as follows:

$$\overline{\overline{G}}_{\rm ee}(z,z',\omega)\mathbf{v}_n = \frac{g_n(z,z',\omega)}{\Gamma\Lambda_n e^{2ikh}-1}\mathbf{v}_n \quad (n=1,2), \tag{12a}$$

$$g_n(z,z',\omega) = \begin{cases} \frac{\eta e^{ikh}}{2i\omega\mu_0}\left[e^{ik(z-z_1)}\Gamma + e^{-ik(z-z_1)}\right]\left[e^{-ik(z'-z_2)}\Lambda_n + e^{ik(z'-z_2)}\right] & z \in (z_1,z'), \\ \frac{\eta e^{ikh}}{2i\omega\mu_0}\left[e^{ik(z'-z_1)}\Gamma + e^{-ik(z'-z_1)}\right]\left[e^{-ik(z-z_2)}\Lambda_n + e^{ik(z-z_2)}\right] & z \in (z',z_2), \end{cases} \tag{12b}$$

#158662 - $15.00 USD Received 23 Nov 2011; revised 11 Jan 2012; accepted 11 Jan 2012; published 19 Jan 2012

where $g_n(z,z',\omega)$ is a regular scalar function. With the right frequency ω and gain effect, the magnitude of the denominator $|\Gamma\Lambda_n \exp(2ikh)-1|$ in Eq. (12a) can be small, indicating huge responses for $\mathbf{v}_{1,2}$. This is just the round-trip oscillation condition of FP modes. Thus, if $\mathbf{J}_s(z,\omega)$ contains the components of $\mathbf{v}_{1,2}$, these components would be significantly induced on $\mathbf{E}(z,\omega)$.

A seeming paradox is related to the identical SPE rates in Eq. (2) and polarization states $\mathbf{v}_{1,2}$ ($\mathbf{u}_{1,2}$) in Eq. (6b) [Eq. (6c)]: the polarization states of resonant cavity modes both resemble one of the two circular polarizations and should solely favor the SPEs from the CP dipole with the same spin orientation (Purcell effect), but in fact, both types of CP dipoles have the identical SPE rates, as indicated in Eq. (2). The paradox originates from the inconsistency between the SPE calculations based on the dyadic Green's function $\overline{\overline{G}}_{\text{ee}}(\mathbf{r},\mathbf{r}',\omega)$ and Fermi's golden rule. In fact, Fermi's Golden rule (Purcell effect) fails to take into account the condition that the polarization of spontaneously-emitted photons from the opposite-oriented CP dipoles can be partially converted to those of resonant cavity modes by reflector 2 when the photons are reflected. Thus, SPEs from those opposite-oriented CP dipoles are not inhibited. In other words, while Fermi's golden rule always requires angular momentum conservations for both SPEs and STEs in radiative transitions, this conservation law only applies to STEs in chiral (anisotropic) cavities because the STE effect is a duplication process of photons. The spontaneously-emitted photons can acquire additional angular momenta from chiral (anisotropic) structures, and the emissions are not limited by angular momentum conservations in radiative transitions.

4. Construction of the chiral cavity

To implement the FP cavity, we use a quarter wavelength distributed Bragg reflector ($\lambda/4$ DBR) with a high reflectivity in its stop band as reflector 1 and the cascaded structure of a $\lambda/4$ DBR and CLC as reflector 2, as shown in Figs. 3(a) and 3(b), respectively. Thus, the reflector (cavity) is chiral. The DBR insertion in reflector 2 is critical. Although CLCs alone satisfy the matrix-element condition of $|(a-b)/2 \mp ic| \ll |a-b|$ for $\overline{\overline{r}}_2$, their characteristic of $a \approx -b$ leads to small magnitudes $|\Lambda_{1,2}|$ and makes the resonance condition $\Gamma\Lambda_{1,2}\exp(2ikh) \approx 1$ difficult. The additional insertion of DBR boosts $|\Lambda_{1,2}|$ (despite the smaller margin $|a-b|$ for the goal condition) and makes lasing easier.

In the calculations, we set the DBR center wavelength to 850 nm. The refractive indices of the high- and low-index regions in both DBRs are assumed nondispersive with values 3.8 and 3.4, respectively. The thicknesses of the two regions are one quarter of the center wavelength divided by the corresponding refractive indices. Reflector 1 (2) has 15 (7) DBR pairs. For the CLC, the ordinary (extraordinary) refractive index n_{o} (n_{e}) is 1.55 (1.65). We choose a chiral pitch of 531.25 nm to match the 850 nm wavelength due to the possibility of near-infrared lasing in CLCs [35]. The number of pitches is 20. Outside reflectors 1 and 2 are two free spaces with refractive indices of 3.5 and 1.6, respectively. In the FP cavity, the complex refractive index of the gain medium is also frequency-independent with a value $3.5-0.0118i$. The cavity length h is 486.3 nm.

The reflectivity spectrum of reflector 1 in Fig. 4(a) is calculated with the transfer-matrix method. The DBR has a high reflection ($|\Gamma|^2 > 99.3$ %) near 850 nm. Similarly, we obtain the reflection matrix of $\overline{\overline{r}}_2$ from propagation matrices of the CLC and DBR [36]. Due to the reciprocity in Eq. (5a) and (5b), the two diagonal matrix elements of $\overline{\overline{r}}_{2,\text{CP}}$ must be identical, reflecting the identical spectra of the square magnitudes for these two matrix elements in the upper graph of Fig. 4(b). In contrast, the square magnitude $|r_{2,\text{CP},+,-}|^2$ is much larger than $|r_{2,\text{CP},-,+}|^2$ [lower graph of Fig. 4(b)], which is the criterion for the resemblance between two polarizations $\mathbf{u}_{1,2}$ and $\hat{e}_+$ (case II). From the two reflection matrices, we calculate the Stokes parameters inside the FP cavity in Fig. 5. The two peaks on the spectra correspond to the FP modes of $\mathbf{u}_1$ and $\mathbf{u}_2$ while the patterns in the z direction reflect the standing waves of the cavity

#158662 - $15.00 USD Received 23 Nov 2011; revised 11 Jan 2012; accepted 11 Jan 2012; published 19 Jan 2012

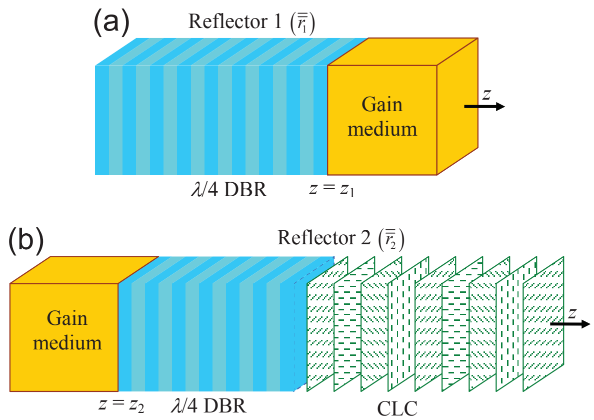

Fig. 3. (a) Reflector 1 is a $\lambda/4$ DBR at the left side of the gain medium. (b) Reflector 2 is the cascade of a $\lambda/4$ DBR and CLC at the right side of the gain medium.

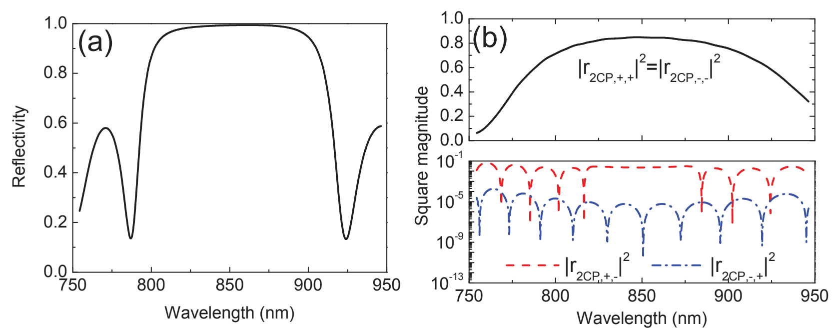

Fig. 4. (a) The reflectivity of reflector 1 versus the wavelength. (b) The square magnitudes of matrix elements in $\bar{\bar{r}}_2$ versus the wavelength. The square magnitudes $|r_{2,\mathrm{CP},+,+}|^2$ and $|r_{2,\mathrm{CP},-,-}|^2$ are equal (upper graph), while $|r_{2,\mathrm{CP},+,-}|^2$ is much larger than $|r_{2,\mathrm{CP},-,+}|^2$ near 850 nm (lower graph).

modes. The magnitudes of $\langle S_1(z,\omega)\rangle$ and $\langle S_2(z,\omega)\rangle$ are smaller than those of $\langle S_0(z,\omega)\rangle$ and $\langle S_3(z,\omega)\rangle$ by about two orders of magnitude, indicating an almost perfect CP field. The ratio $\langle S_3(z,\omega)\rangle/\langle S_0(z,\omega)\rangle$ is an indicator of the degree of circular polarization, and its maximum value at the main FP peak is about 99.8 % inside the cavity. Since we adopt an isotropic gain and a SPE source which does not favor particular CP emissions, an intrinsically reciprocal but chiral cavity is sufficient for the stimulated emission of photons in a nearly pure spin state. The transmission out of the isotropic reflector preserves the polarization state inside the cavity, and a nearly perfect CP radiation should be observable outside reflector 1.

5. Effect of circularly-polarized stimulated emissions on reciprocity

If the gain medium consists of emitter systems which contain degenerate time-reversal paired states, the STEs in this chiral FP cavity can make the occupation numbers of the time-reversal pairs uneven. This effect may further change the appearance of the permittivity tensor. In particular, the dressed permittivity tensor represented in a real orthonormal basis set may become nonsymmetric, which breaks the reciprocity of the cavity.

To see the origin of this phenomenon, we use a simple model of double two-level systems

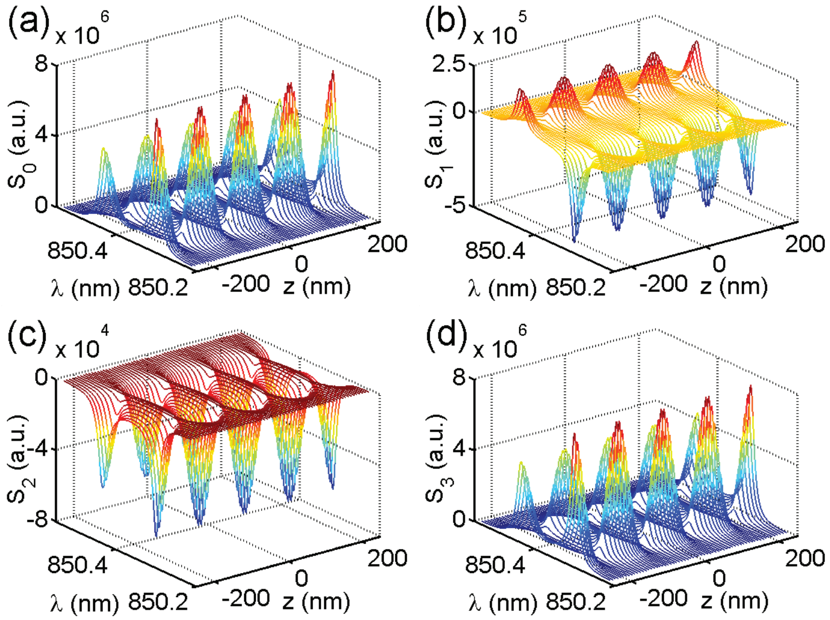

Fig. 5. (a)–(d) Spectra of the Stokes parameters $\langle S_n(z,\omega)\rangle$ $(n = 0-3)$. The magnitudes of $\langle S_1(z,\omega)\rangle$ and $\langle S_2(z,\omega)\rangle$ are much smaller than those of $\langle S_0(z,\omega)\rangle$ and $\langle S_3(z,\omega)\rangle$.

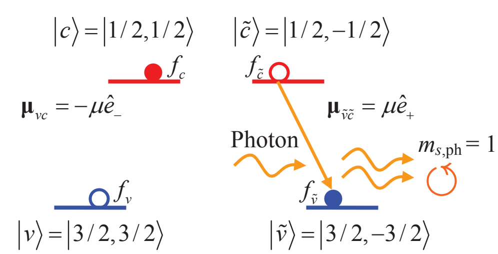

Fig. 6. The energy levels of double two-level systems forming a time-reversal pair. The dipole moment $\boldsymbol{\mu}_{vc}$ between states c ($|1/2,1/2\rangle$) and v ($|3/2,3/2\rangle$) is $-\mu\hat{e}_-$ and that $\boldsymbol{\mu}_{\tilde{v}\tilde{c}}$ between $\tilde{c}$ ($|1/2,-1/2\rangle$) and $\tilde{v}$ ($|3/2,-3/2\rangle$) is $\mu\hat{e}_+$. Due to the dominance of photons with a spin quantum number $m_{s,\mathrm{ph}} = 1$, only the STEs from $\tilde{c}$ to $\tilde{v}$ take place.

which form a time-reversal pair for the gain medium. As shown in Fig. 6, the excited state c ($\tilde{c}$) is the spin angular momentum eigenstate $|s,m_s\rangle = |1/2,1/2\rangle$ ($|1/2,-1/2\rangle$) with the z angular momentum quantum number $m_s = 1/2$ $(-1/2)$ [the z axis here is identical to that of the chiral FP cavity]. The ground state v ($\tilde{v}$) is the angular momentum state $|j,m\rangle = |3/2,3/2\rangle$ ($|3/2,-3/2\rangle$) with the z angular momentum quantum number $m = 3/2$ $(-3/2)$ in the total angular momentum space $j = 3/2$. The dipole moment $\boldsymbol{\mu}_{vc} = -\mu\hat{e}_-$ ($\boldsymbol{\mu}_{\tilde{v}\tilde{c}} = \mu\hat{e}_+$) between states c and v ($\tilde{c}$ and $\tilde{v}$) is circularly-polarized. Selection rules ensure that radiative transitions from c to v ($\tilde{c}$ to $\tilde{v}$) are only accompanied by free-space photon emissions in the polarization state $\hat{e}_-$ (z spin angular momentum quantum number $m_{s,\mathrm{ph}} = -1$), and those between states $\tilde{c}$ and $\tilde{v}$ result in photon emissions in the polarization state $\hat{e}_+$ ($m_{s,\mathrm{ph}} = 1$). Such examples of the double two-level systems can be the fundamental heavy-hole excitons or the bandedge

#158662 - $15.00 USD Received 23 Nov 2011; revised 11 Jan 2012; accepted 11 Jan 2012; published 19 Jan 2012

states of unstrained or compressively-strained [001] quantum wells [37]. Let us approximate polarization eigenstates $\mathbf{u}_{1,2}$ of the two cavity modes in the chiral FP cavity as $\hat{e}_+$ for simplicity. Since only photons in the polarization state $\hat{e}_+$ experience cavity resonances and dominate in STEs, the population consumption in state $\tilde{c}$ is much faster than that of c. As a result, the occupation number $f_{\tilde{c}}$ of $\tilde{c}$ is smaller than that f_c of c, and the occupation $f_{\tilde{v}}$ of $\tilde{v}$ is larger than the counterpart f_v of v. This unbalance in state occupations leads to unequal occupation differences: $f_v - f_c \neq f_{\tilde{v}} - f_{\tilde{c}}$, which is the sign of T-symmetry breaking.

From the density-matrix formalism [37] and the assumption that the double two-level systems remain degenerate except for state occupations, the effective permittivity tensor $\overline{\overline{\varepsilon}}_{\mathrm{r}}(\omega)$ due to the feedback from the CP STEs can be written as

$$\overline{\overline{\varepsilon}}_{\mathrm{r}}(\omega) = \varepsilon_{\mathrm{r,bgd}} \overline{\overline{I}}_3 + \frac{N_{\mathrm{e}}}{\hbar\varepsilon_0} \frac{1}{\omega_{cv} - \omega - i\gamma_{cv}} \left[\boldsymbol{\mu}_{vc}\boldsymbol{\mu}_{vc}^{\dagger}(f_v - f_c) + \boldsymbol{\mu}_{\tilde{v}\tilde{c}}\boldsymbol{\mu}_{\tilde{v}\tilde{c}}^{\dagger}(f_{\tilde{v}} - f_{\tilde{c}}) \right], \tag{13a}$$

where $\varepsilon_{\mathrm{r,bgd}}$ is the background permittivity; N_{e} is the volume density of emitters; and γ_{cv} is the dephasing parameter for the radiative transition between states c and v. If we substitute the expressions of dipole moments $\boldsymbol{\mu}_{vc} = -\mu\hat{e}_-$ and $\boldsymbol{\mu}_{\tilde{v}\tilde{c}} = \mu\hat{e}_+$ into Eq. (13a) and represent $\overline{\overline{\varepsilon}}_{\mathrm{r}}(\omega)$ in the basis set $\{\hat{x}, \hat{y}, \hat{z}\}$, the matrix form of $\overline{\overline{\varepsilon}}_{\mathrm{r}}(\omega)$ becomes

$$\begin{aligned} \overline{\overline{\varepsilon}}_{\mathrm{r}}(\omega) = \varepsilon_{\mathrm{r,bgd}} \overline{\overline{I}}_3 + \frac{N_{\mathrm{e}}}{\hbar\varepsilon_0} \frac{\mu^2}{\omega_{cv} - \omega - i\gamma_{cv}} \Bigg\{ & \frac{[(f_v - f_c) + (f_{\tilde{v}} - f_{\tilde{c}})]}{2} \begin{pmatrix} \overline{\overline{I}}_2, & \mathbf{0}_{2\times1} \\ \mathbf{0}_{1\times2}, & 0 \end{pmatrix} \\ & + \frac{[(f_v - f_c) - (f_{\tilde{v}} - f_{\tilde{c}})]}{2} \begin{pmatrix} -\overline{\overline{\sigma}}_2, & \mathbf{0}_{2\times1} \\ \mathbf{0}_{1\times2}, & 0 \end{pmatrix} \Bigg\}, \end{aligned} \tag{13b}$$

where $\mathbf{0}_{2\times1}$ ($\mathbf{0}_{1\times2}$) is the 2-by-1 (1-by-2) null matrix. If $f_v - f_c \neq f_{\tilde{v}} - f_{\tilde{c}}$, the antisymmetric Pauli matrix $\overline{\overline{\sigma}}_2$ makes the permittivity tensor $\overline{\overline{\varepsilon}}_{\mathrm{r}}(\omega)$ nonsymmetric and turns the chiral FP cavity nonreciprocal. In fact, the matrix form of $\overline{\overline{\varepsilon}}_{\mathrm{r}}(\omega)$ is similar to the permittivity tensor in the presence of the magneto-optical effect, which explicitly breaks the reciprocity.

In Eq. (13b), the asymmetry of the permittivity tensor vanishes in the quasi equilibrium condition: $f_v - f_c \approx f_{\tilde{v}} - f_{\tilde{c}}$, which is often equivalent to $f_c \approx f_{\tilde{c}}$ and $f_v \approx f_{\tilde{v}}$. Unless the occupations relax rapidly between angular momentum states forming time-reversal pairs, namely, fast angular momentum relaxation, the reciprocity is generally broken in this chiral FP cavity. In principle, the model in sections 3 and 4 should take this nonreciprocal effect into account. Nevertheless, the calculations based on reciprocal cavities and reasoning from Eq. (13a) and (13b) indicate that the reciprocity (in a generalized sense for lasers) may be unstable in the presence of both chirality and gain.

6. Conclusion

In summary, we have analyzed the criterion of the T-symmetry breaking of the emitter state in absence of imposed nonreciprocal environments, and proposed a prototype of reciprocal FP cavities which make the stimulated emission of photons directly in a nearly pure spin state possible. Due to the special chiral reflector, which is constructed with a $\lambda/4$ DBR and CLC, the potential lasing modes only have polarization states close to one of the circular polarizations. In this case, chirality in turn may lead to a nonreciprocal cavity via the CP stimulated emission.

Acknowledgments

This work is funded by the research project of Research Center for Applied Sciences, Academia Sinica, Taiwan, and support from National Science Council, Taiwan, under grant No. NSC100-2112-M-001-002-MY2.

#158662 - $15.00 USD Received 23 Nov 2011; revised 11 Jan 2012; accepted 11 Jan 2012; published 19 Jan 2012